

Opinion

# Tissue Iron in Friedreich Ataxia

Arnulf H Koeppen<sup>1,\*</sup><sup>1</sup>Research Service (151), VA Medical Center, Albany, NY 12208, USA\*Correspondence: [arnulf.koeppen@med.va.gov](mailto:arnulf.koeppen@med.va.gov) (Arnulf H Koeppen)

Academic Editor: Gernot Riedel

Submitted: 6 July 2023 Revised: 19 August 2023 Accepted: 23 August 2023 Published: 10 January 2024

## Abstract

Heart, dentate nucleus, and dorsal root ganglia (DRG) are targets of tissue damage in Friedreich ataxia (FA). This report summarizes the histology and histopathology of iron in the main tissues affected by FA. None of the affected anatomical sites reveals an elevation of total iron levels. In the myocardium, a small percentage of fibers shows iron-reactive granular inclusions. The accumulation of larger iron aggregates and fiber invasion cause necrosis and damage to the contractile apparatus. In the dentate nucleus, the principal FA-caused tissue injury is neuronal atrophy and grumose reaction. X-ray fluorescence mapping of iron in the dentate nucleus in FA shows retention of the metal in the center of the collapsed structure. Immunohistochemistry of ferritin, a surrogate marker of tissue iron, confirms strong expression in oligodendrocytes of the efferent white matter of the dentate nucleus and abundance of ferritin-positive microglia in the atrophic gray matter. Iron dysmetabolism in DRG is complex and consists of prominent expression of ferritin in hyperplastic satellite cells and residual nodules, also a loss of the iron export protein ferroportin from the cytoplasm of the remaining DRG nerve cells.

**Keywords:** friedreich ataxia; ferritin; iron; mitochondrial ferritin; ferroportin; cardiomyopathy; atrophy; dorsal root ganglia

## 1. Introduction

The story of iron, and specifically biological iron, in Friedreich ataxia (FA) began in 1980 when Lamarche *et al.* [1] reported the presence of granular iron in the myocardium of three patients with FA. This early paper gained additional significance with the discovery of the mutation in FA [2] and the deficiency of frataxin, a protein that is now often called an iron chaperone but the role of which is rather more complex [3]. At first, FA was considered a new form of hemochromatosis, but it became apparent that iron deposits were restricted to the heart, contrasting with other forms of hereditary iron overload. Nevertheless, two groups of researchers reported iron excess in the dentate nucleus of FA patients, based on the paramagnetic effect of the metal on magnetic resonance signals [4,5]. The dentate nucleus is a prominent target of FA, and it seemed reasonable to attempt iron chelation with deferiprone, a chelator that passes the blood-brain barrier [5]. While some students of FA remain enthusiastic over the role of iron in the pathogenesis of FA, iron chelation is no longer considered a suitable therapy of the disease. This brief report summarizes the putative role of iron in the pathogenesis of FA cardiomyopathy and the major sites of FA-induced damage of the nervous system, namely, dentate nucleus and dorsal root ganglia (DRG).

## 2. Heart Iron in FA

Fig. 1A,B show the iron histochemistry of 2 sections of the heart in an FA patient. Fig. 1A represents an endocardial biopsy of the patient obtained at age 9. Fig. 1B shows

the iron reaction in an autopsy specimen of the same patient who succumbed to FA cardiomyopathy at the age of 26 years. The comparison allows the conclusion that the formation of granular iron in cardiomyocytes occurs in the early life of an FA patient and does not reflect disease duration [6]. Dr Lamarche of the Centre Hospitalier Universitaire de Sherbrooke in Sherbrooke, Quebec, Canada, assayed total heart iron in 9 patients with FA but did not find a significant elevation compared to control hearts. He sent his results to the author's laboratory in Albany, NY, USA where they were compared with iron assays of 9 additional FA heart specimens. Despite different colorimetric assay methods, the results were very similar, namely,  $30.7 \pm 19.3$  mg/100 mg dry weight (mean  $\pm$  standard deviation [SD]). In 11 normal control heart specimens, total iron levels were  $31.3 \pm 24.1$  mg/100 mg dry weight [6]. Michael *et al.* [6] also determined total ferritin in extracts of frozen samples of left ventricular walls by enzyme-linked immunosorbent assay and discovered no significant differences between FA hearts ( $230 \pm 172$   $\mu$ g/gram wet weight [mean  $\pm$  SD]) and normal controls ( $148 \pm 86$   $\mu$ g/gram wet weight [mean  $\pm$  SD]). Western blots of heart ferritin in some, but not all, FA cases showed upregulation of the light ferritin subunit [6]. Electron microscopy of FA heart after preincubation of the sections with bismuth subnitrate showed ferritin aggregates in mitochondria (Fig. 2) [6]. Through the courtesy of Drs Sonia Levi and Paolo Santambrogio, San Raffaele Research Institute, Milan, Italy, the author received a monoclonal antibody to mitochondrial ferritin. Immunohistochemistry with this antibody showed reaction product in a percentage of cardiomyocytes. For a while, it seemed



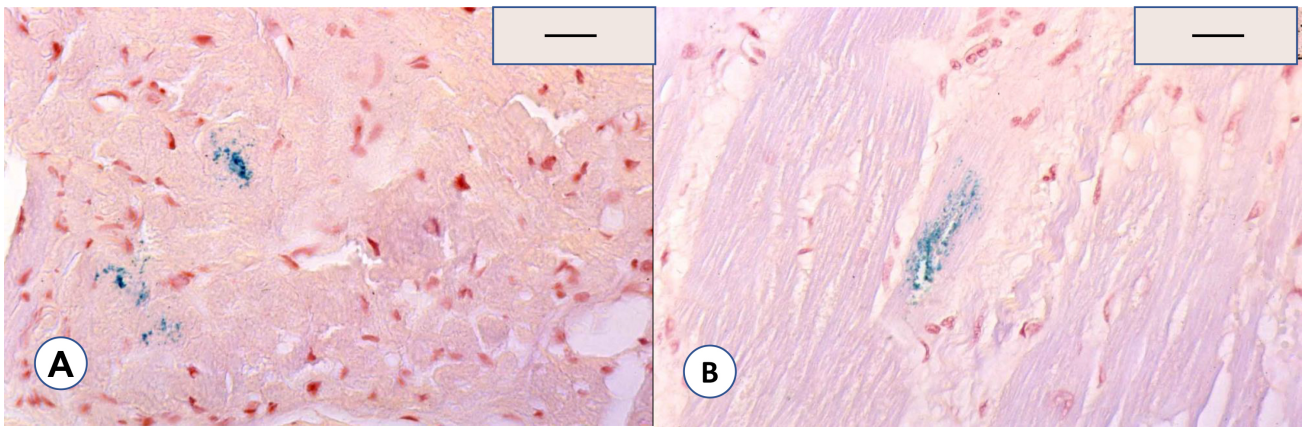


**Fig. 1. Iron histochemistry of the heart in FA.** The patient was a female who had an endocardial biopsy at the age of 9 years (A) and died at the age 26 years (B). Perl's iron stain shows finely granular blue inclusions in a small percentage of heart fibers. The counterstain is Brazilin. Bars, 50  $\mu$ m. FA, Friedreich ataxia.

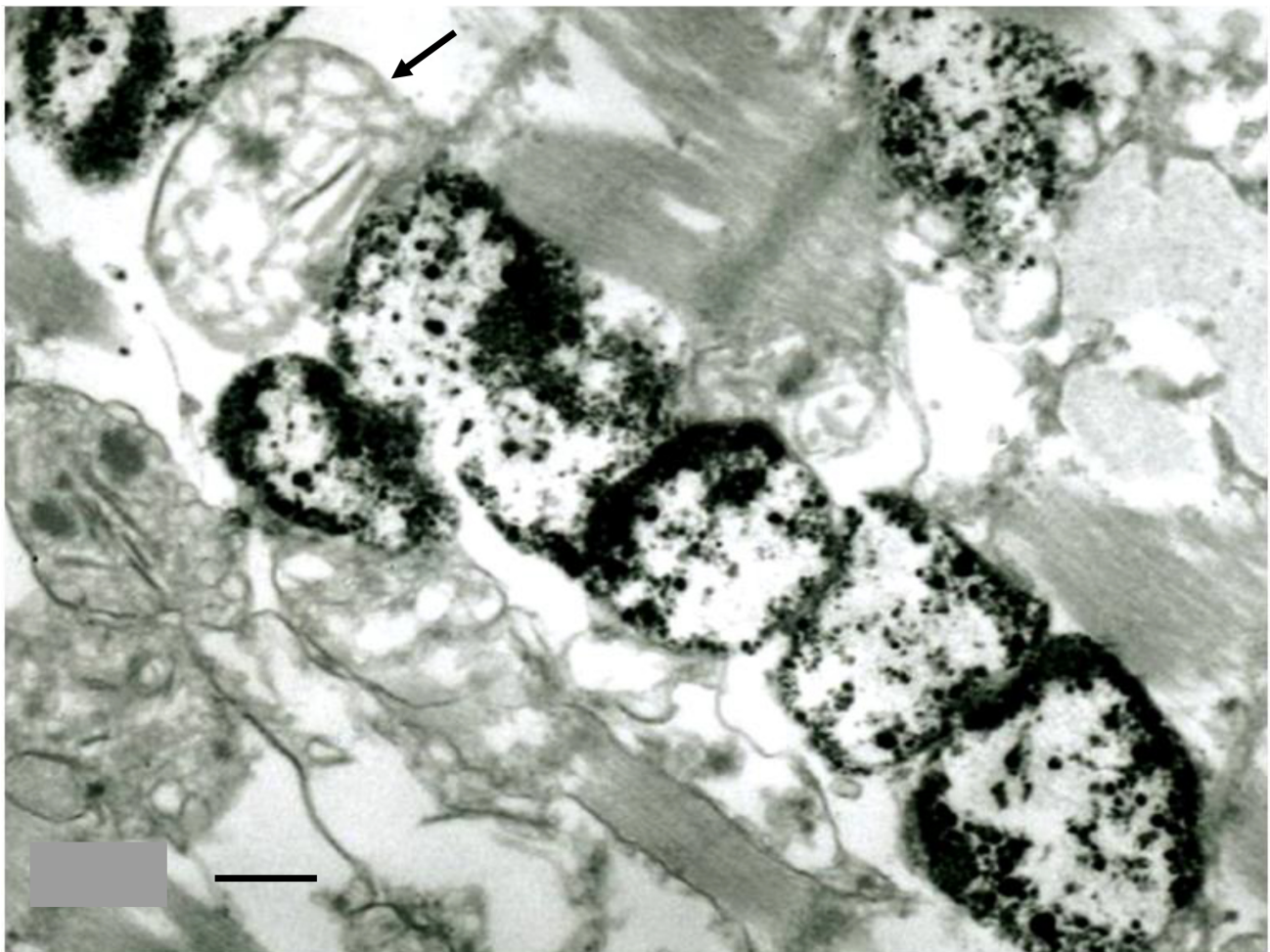


**Fig. 2. Mitochondrial ferritin in the heart of FA.** Sections were incubated with bismuth subnitrate to identify ferritin. All electron-opaque inclusions in mitochondria represent ferritin because other contrasting agents, such as uranyl acetate and osmium were omitted. The arrow indicates a mitochondrion without ferritin inclusions. Bar, 1  $\mu$ m.

that the very focal iron excess in FA hearts was restricted to mitochondria. Immunohistochemistry with an antibody to cytosolic holoferitin, however, showed reaction product

in the cytoplasm of heart fibers, with or without colocalization with mitochondrial ferritin [7] (Fig. 3). While total iron in FA cardiomyopathy is not elevated, the inclusions

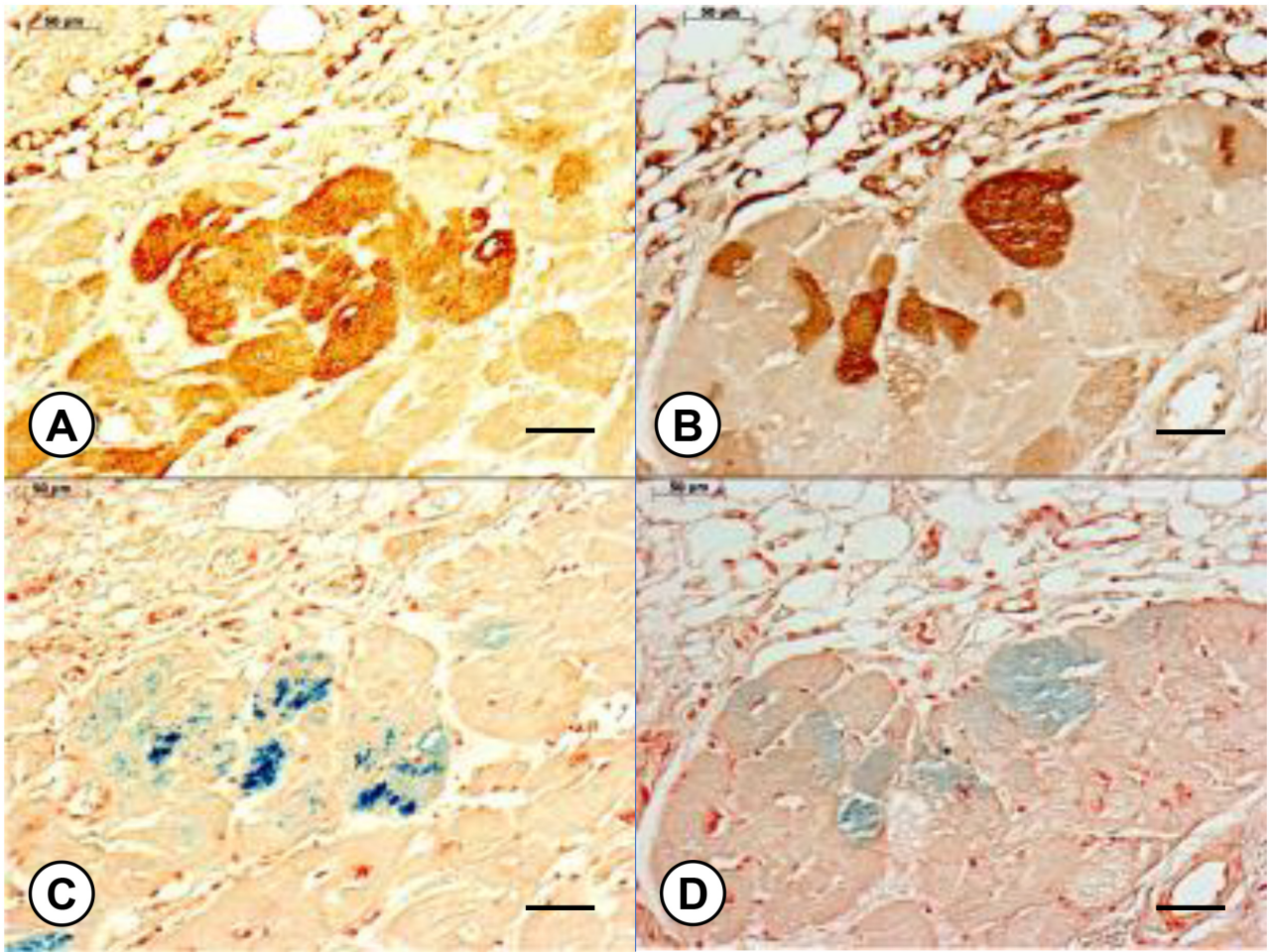


**Fig. 3. Ferritin and mitochondrial ferritin in FA cardiomyopathy.** (A) Cytosolic holoferitin; (B) mitochondrial ferritin; (C) iron in a section adjacent to (A); (D) iron in section adjacent to (B). A cluster of iron-reactive fibers (C) shows strong expression of holoferitin (A). The iron-containing fibers in (D) are reactive for mitochondrial ferritin (B). Bars, 50 µm.



**Fig. 4. Iron, ferroportin, and holoferitin in a necrotic heart fibers.** Iron histochemistry (A); immunohistochemistry for ferroportin (B) and holoferitin (C). The heart fiber in (A) contains clumps of aggregated iron. In an adjacent section (B), the same fiber shows no ferroportin reaction product but is strongly reactive for ferritin (C). Bars, 10 µm.

of iron-reactive granules in cardiomyocytes is not a benign process. Progressive accumulation leads to fiber necrosis, invasion by macrophages and destruction of the contractile apparatus of the heart [7]. Iron-laden fibers display a deficiency in ferroportin, the principal iron exporter in most

cells (Fig. 4). From the illustration (Fig. 4), it cannot be concluded that ferroportin deficiency in the cardiomyocyte antedates the iron overload. It is equally possible that the destruction of the cytoplasm caused the disappearance of ferroportin. In support of a ferroportin deficiency before

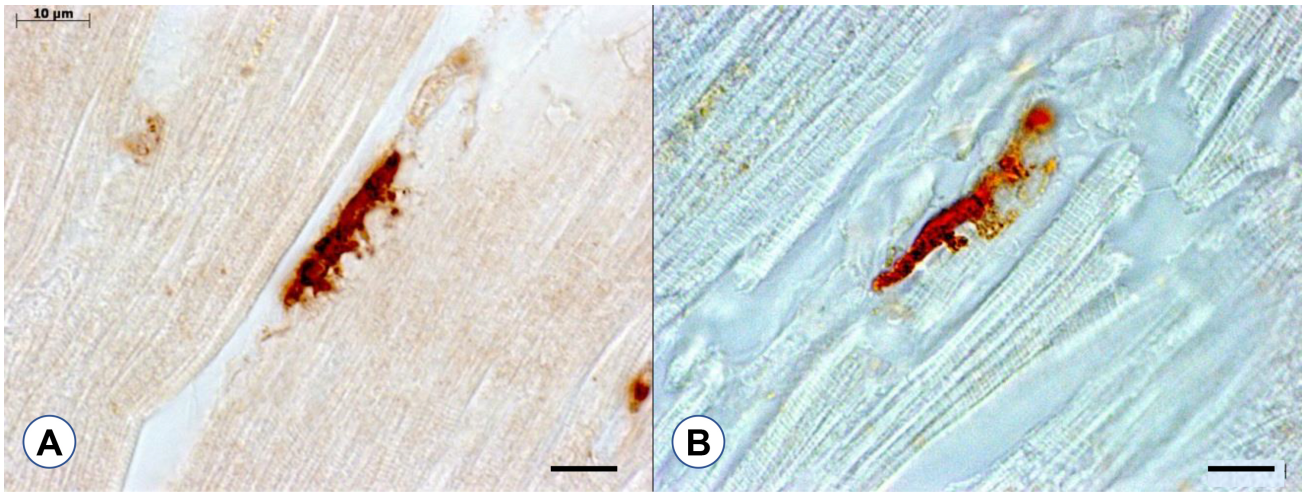


**Fig. 5. Attachment of monocytes to cardiomyocytes.** (A) Immunohistochemistry for CD68; (B) immunohistochemistry for hepcidin. (A) A CD68-reactive monocyte is projecting delicate processes toward the interior of a cardiomyocyte. (B) A hepcidin-reactive monocyte shows similar projections toward a heart fiber where interaction with ferroportin may take place. Bars, 10 µm. Figures from reference [7]. Reproduced with permission from Koeppen AH, The pathogenesis of cardiomyopathy in Friedreich ataxia. PLoS ONE. 2015. [7].

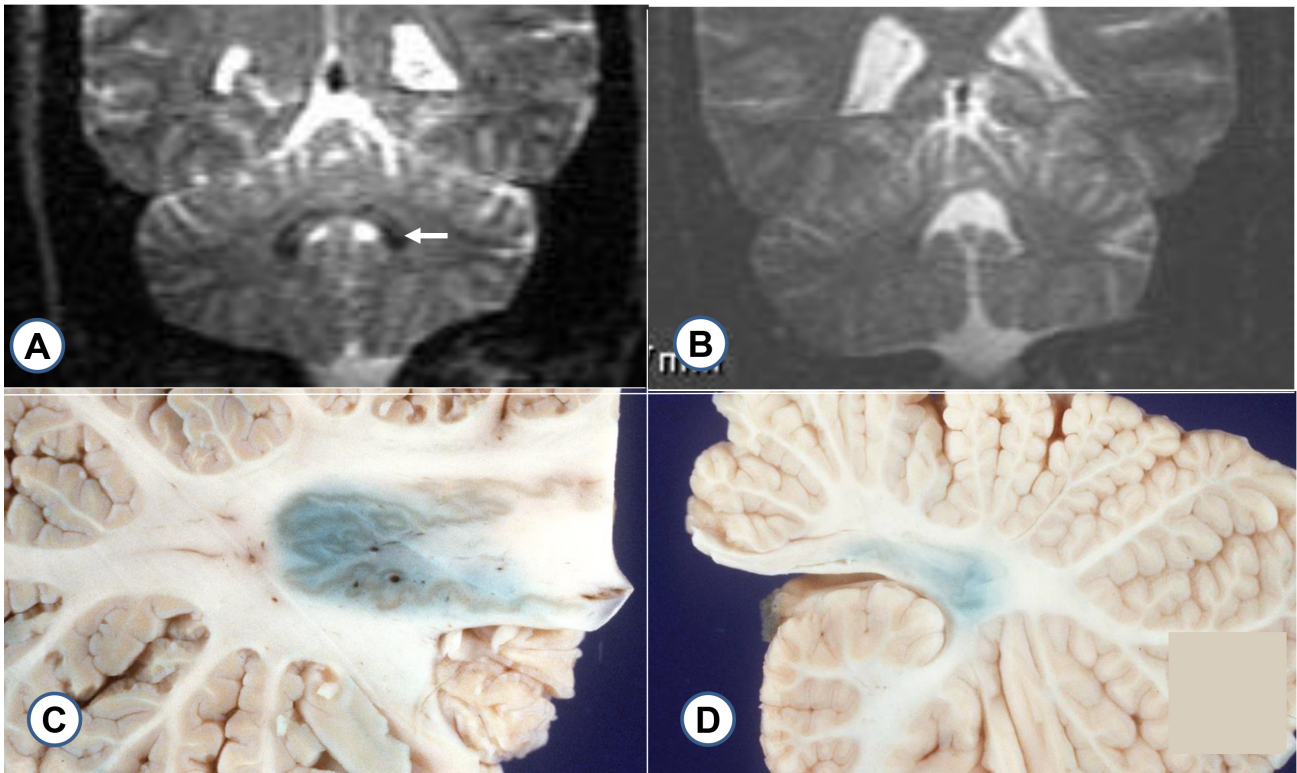


**Fig. 6. Magnetic resonance images of the dentate nucleus in FA and a control; macrostain of iron in formalin-fixed cerebellum.** (A) T2 weighted image of a control dentate nucleus (arrow); (B) FA; (C) macrostain for iron in a normal dentate nucleus; (D) FA. (A) The arrow shows the outline of the iron-rich normal dentate nucleus; (B) In FA, the paramagnetic effect of iron in the dentate nucleus has become indistinct. (C) and (D) Slices of cerebellum were overlaid with Perls's [8] reagents. The normal specimen (A) shows the outline of the gray matter ribbon and a more diffuse reaction product. In FA (B), only some diffuse reaction product remains. The gray matter of the dentate nucleus is no longer distinct.

iron overload, however, an antibody to hepcidin, a master control protein of iron metabolism, shows expression

of hepcidin-reactive macrophages that attach to the plasma membrane of cardiomyocytes and seemingly penetrate into

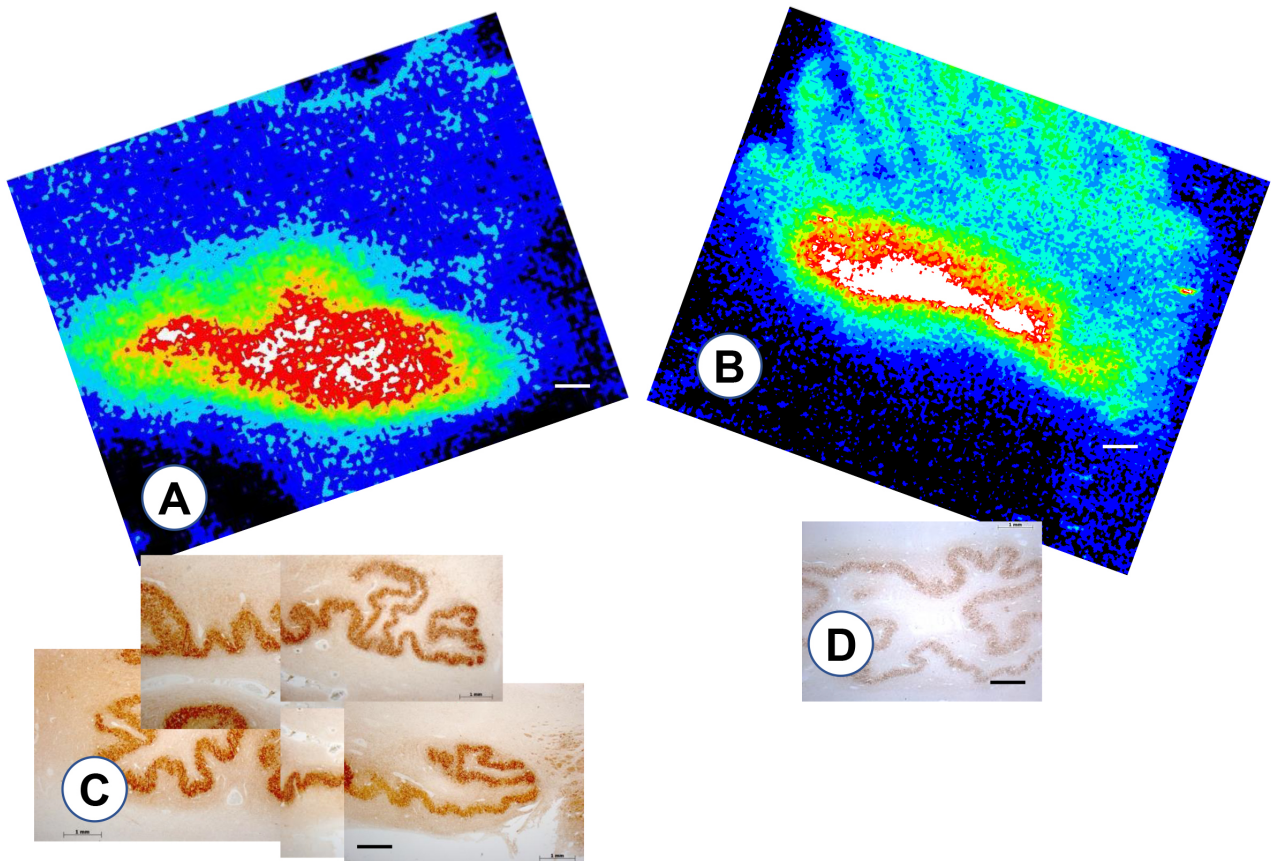


**Fig. 7. X-ray fluorescence mapping of iron in a normal dentate nucleus and the dentate nucleus of FA; matching immunohistochemistry of glutamic acid decarboxylase in the normal dentate nucleus and in FA.** (A) normal dentate nucleus; (B) dentate nucleus in FA; (C) normal dentate nucleus, immunohistochemistry of glutamic acid decarboxylase; (D) dentate nucleus in FA, immunohistochemistry of glutamic acid decarboxylase. Iron fluorescence in (A) and (B) is given in pseudo colors. Maximum signal is shown as white; declining intensities are presented in red, yellow, and green, respectively. In FA, the overall size of the dentate nucleus is smaller, but maximum iron fluorescence is concentrated in the center of the nucleus. The matching composite images of glutamic decarboxylase (A,B) show simplification of the dentate nucleus in FA (D). Iron fluorescence does not match the gray matter ribbon of the dentate nucleus in the control specimen (C) or the sample of FA (D). Bars, 1 mm.

the cardiomyocyte (Fig. 5, Ref. [7]). At this location, hepcidin destroys ferroportin and thereby hinders the *exit* of iron from heart fibers. Based on these observations, Koepen *et al.* [7] tentatively concluded that the accumulation of iron in FA heart fibers is due to failed iron export rather than accelerated iron entry.

### 3. Iron in the Dentate Nucleus in FA

The dentate nucleus is naturally rich in iron, and, based on the paramagnetic effect of the metal, T2-weighted magnetic resonance images show the nucleus in the cerebellum to advantage (Fig. 6C,D). Contrary to Waldvogel *et al.* [4] and Boddart, *et al.* [5], however, the author asserts that Friedreich ataxia causes shrinkage of the dentate nucleus and reduced paramagnetic iron effect (Fig. 6). Fig. 6 shows macroscopic iron stains of the dentate nucleus in FA (Fig. 6B) and a control specimen (Fig. 6A). Perls's

[8] iron stain generates a crisp outline of the normal meandering gray matter ribbon (Fig. 6A) while the blue reaction product in FA is consistent with a globular collapse of the dentate nucleus (Fig. 6D). The macroscopic iron stain is misleading as systematic chemical assay of iron in digests of 9 dentate nuclei and 9 control specimens showed no difference in the levels of the metal [9]. Dentate iron levels in FA were  $1.53 \pm 0.53$   $\mu\text{mole/gram}$  wet weight (mean  $\pm$  standard deviation). In control samples, the iron levels were  $1.78 \pm 0.88$   $\mu\text{mole/gram}$  wet weight. Ferritin as a surrogate marker of tissue iron, was similarly unchanged in FA:  $206.9 \pm 46.6$   $\mu\text{g/gram}$  wet weight in FA and  $210.9 \pm 9$   $\mu\text{g/gram}$  wet weight in controls. A minor effect of Fe dysmetabolism in FA was the upregulation of L-ferritin [9]. A new method, non-destructive tissue mapping by X-ray fluorescence gave additional information on iron in the dentate nucleus [10]. Peak iron X-ray fluorescence arose from the white matter in the center of the dentate nucleus and did not colocalize

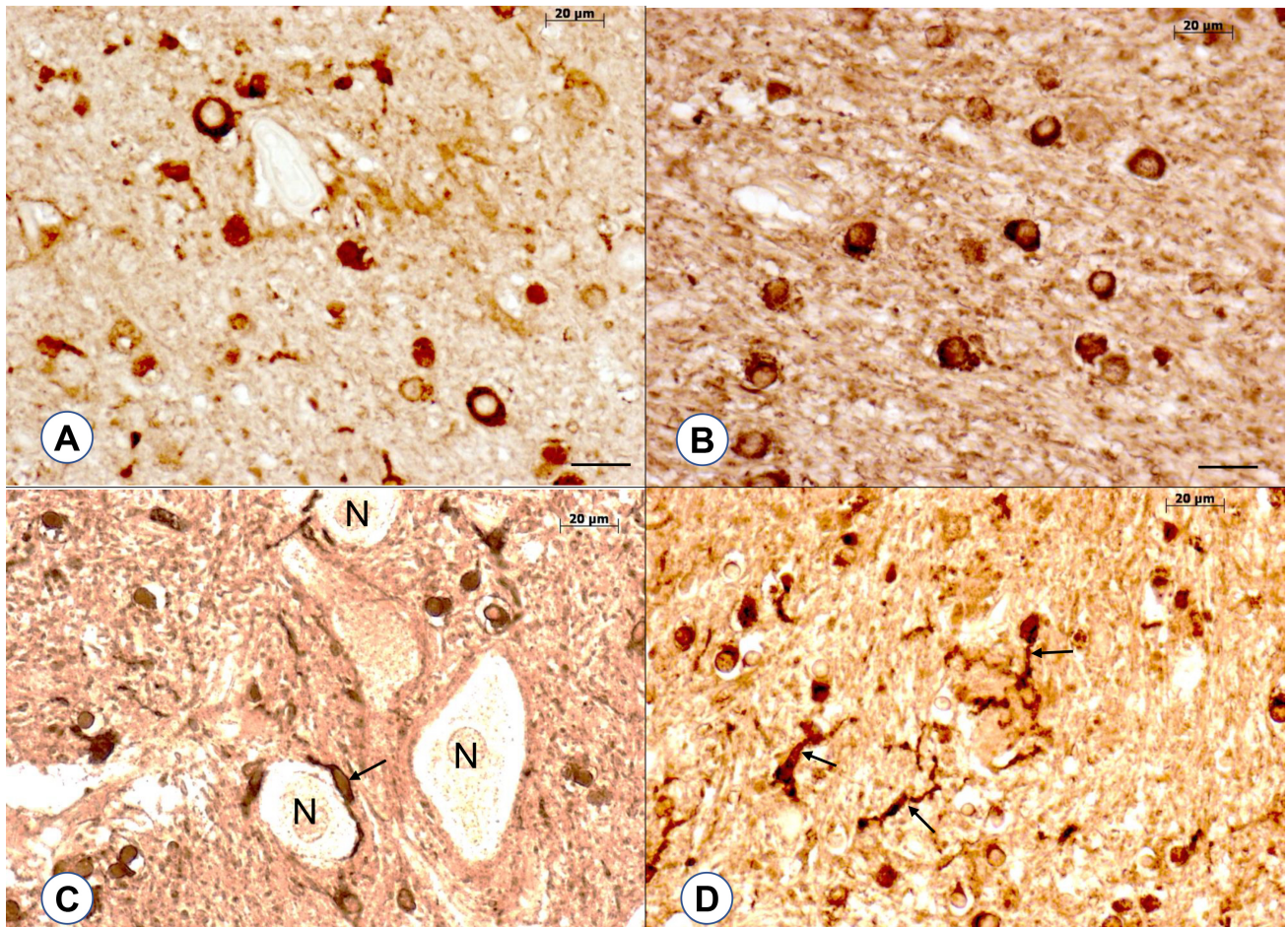


**Fig. 8. Ferritin in the efferent white matter tract of the dentate nucleus in a control and in FA.** (A) control dentate nucleus; (B) FA. (C) normal dentate gray matter, immunohistochemistry of holoferritin; (D) dentate nucleus in FA; immunohistochemistry of holoferritin. In the efferent myelinated fiber tract of the dentate nucleus, ferritin reaction product identifies the reactive cells as oligodendroglia (A). In FA, the main site of ferritin remains oligodendroglia (B), but the reactive cells are smaller than in the normal control (A). In the normal dentate gray matter, ferritin is expressed in juxtaneuronal microglia (C, arrow) and other small cells (C); in the atrophic dentate nucleus of FA, ferritin reaction product shows more abundant microglia (D, arrows). N, neurons; Bars, 20 µm.

with the gray matter ribbon (Fig. 7A). In FA, maximum iron signal was also present in the center of the atrophic dentate nucleus (Fig. 7B). Quantification of iron in zones of the dentate nucleus, based on pseudocolors, yielded concentrations in normal dentate nuclei from 55 to 364 µg/mL polyethyleneglycol, and from 42 to 344 µg/mL in FA [10]. The embedded tissue samples could be recovered by dissolving polyethyleneglycol in an aqueous buffer. After re-fixing in formaldehyde solution, the recovered tissue were reembedded in paraffin. Sections were stained for glutamic acid decarboxylase (GAD) to visualize the gray matter ribbon of the dentate nucleus (Fig. 7C,D). Matching the iron maps (Fig. 7A,B) with the chain of GAD reaction product confirmed the high iron signal in the white matter of the normal dentate and in the center of the collapsed nucleus in FA (Fig. 7B,D). The macro-stains of iron (Fig. 6A,B) show hazy blue reaction product in the vicinity of the normal gray matter ribbon (Fig. 6A) and through the entire nucleus in

FA (Fig. 6B). This observation is similar to the illustrations published by Spatz in 1922 [11]. While diffusion artifact is a consideration, the blue rim actually has a biological explanation. Stains for ferritin confirm the strong expression of the protein in the cytoplasm of small round cells in the dentate hilus, sometimes called the amiculum (Fig. 8A). From their appearance, these cells are identifiable as oligodendrocytes. In FA, ferritin-reactive oligodendrocytes remain prominent in the amiculum but are distinctly smaller (Fig. 8B). Ferritin-containing cells in the gray matter of the dentate nucleus undergo more modest changes (Fig. 8C,D). The most prominent ferritin-containing cell type is the microglia that often lie adjacent to neurons (Fig. 8C). In FA, the advancing loss of nerve cells in the dentate nucleus is accompanied by a greater abundance of ferritin-reactive microglia (Fig. 8D).

The described systematic analysis of iron and ferritin in the dentate nucleus of control and FA samples prompt the

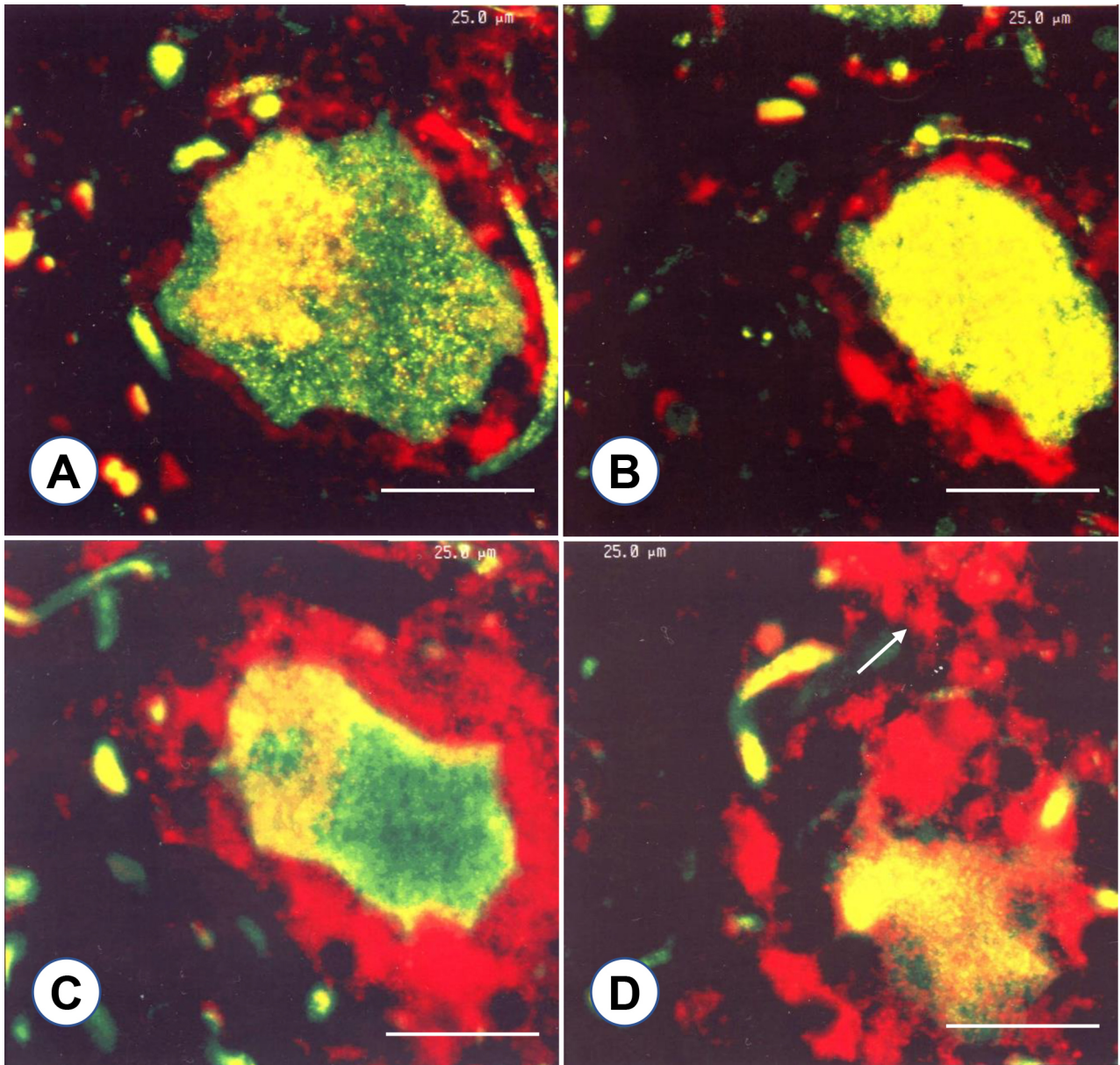


**Fig. 9. Double-label laser scanning confocal immunofluorescence microscopy of class III- $\beta$ -tubulin and holoferritin in DRG of a control and a DRG section of FA.** (A,B) normal DRG; (C,D) FA. Class III- $\beta$ -tubulin is a neuronal marker and shows nerve cells in strong green and yellow fluorescence of fluorescein-isothiocyanate. Cy3 fluorescence reveals ferritin in satellite cells of normal DRG neurons (A,B) and a widened ring of ferritin-positive satellite cells in FA (C,D). Ferritin is also prominent in a residual nodule of FA (D, arrow). Bars, 25  $\mu$ m.

following conclusions: When expressed on the basis of wet weight, the dentate nucleus in FA retains its iron and shifts it to the center of the nucleus. Ferritin is strongly expressed in oligodendrocytes of the amiculum, and these cells remain ferritin-reactive in FA. It is not surprising that the dentate nucleus retains a general property of the mammalian brain, namely, limited iron exit despite the destruction of gray and white matter of the nucleus.

#### 4. Iron in the Dorsal Root Ganglia of FA

Dorsal root ganglia (DRG) are a prominent target of FA, and the lesion accounts for the neuropathy in the disease and the failed development of the dorsal columns of the spinal cord and the dorsal spinocerebellar tracts. Koeppen *et al.* [12] presented morphological evidence that smallness of the DRG in FA constitutes hypoplasia rather than atrophy, but the cellular proliferation of satellite cells and neuronophagia of DRG neurons also point to a delayed destructive process of the remaining nerve cells [13]. Evidence of iron dysmetabolism in DRG of FA is limited. Iron assays

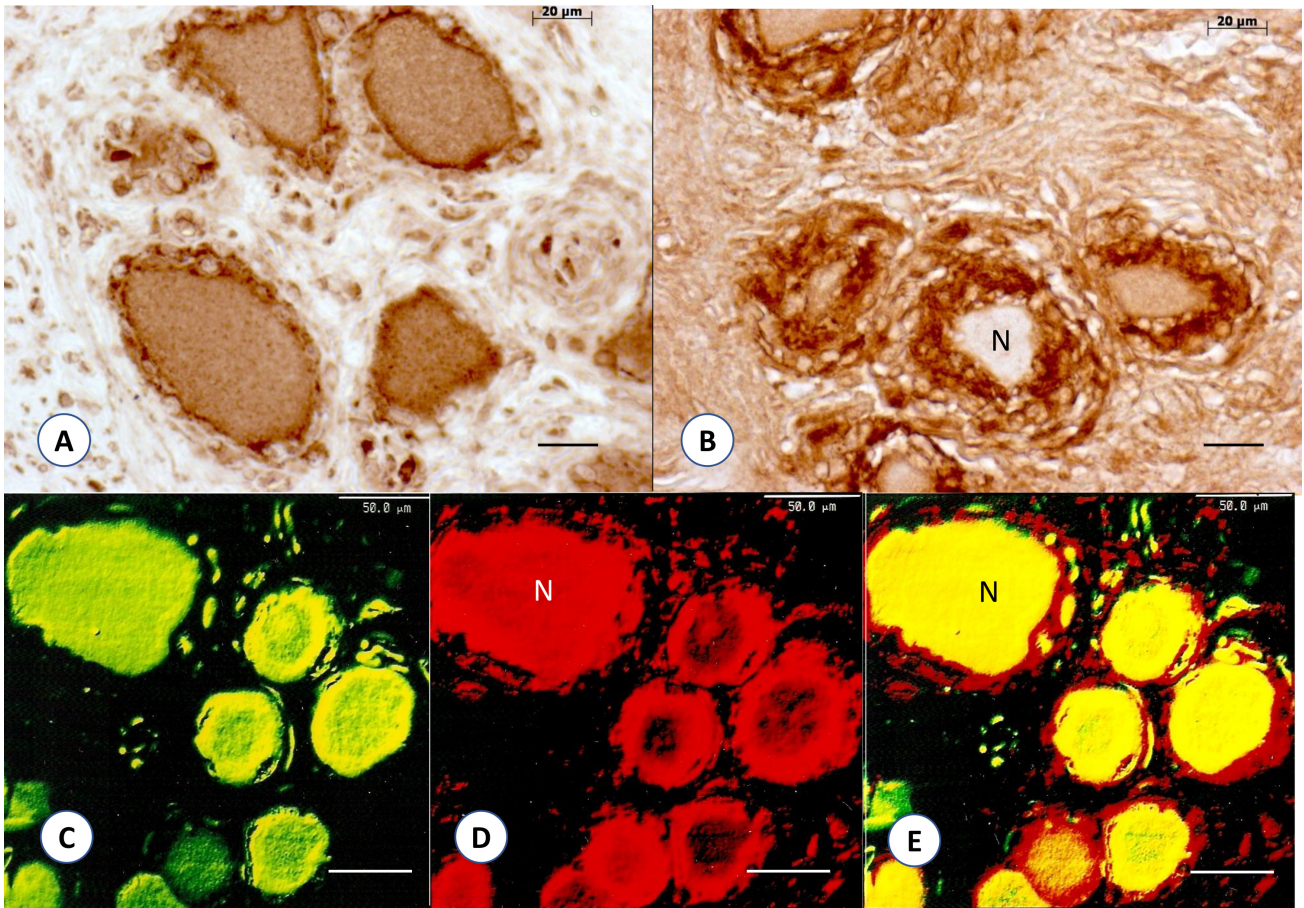


**Fig. 10. Immunohistochemistry and double-label laser scanning confocal immunofluorescence microscopy of ferroportin in DRG.** (A,B) Ferroportin in DRG, immunohistochemistry; (C–E), double-label immunofluorescence microscopy of class III- $\beta$ -tubulin and ferroportin in DRG. (A) Normal DRG; ferroportin reaction product is present in the cytoplasm of neurons and in satellite cells; (B) DRG in FA; ferroportin in FA is strongly expressed in hyperplastic satellite cells and has faded from the cytoplasm of one nerve cell (N). (C–E) DRG neurons in FA. Class III- $\beta$ -tubulin immunofluorescence (fluorescein isothiocyanate) shows the general smallness of the surviving nerve cells (C). Red ferroportin immunofluorescence (Cy3) is prominent in satellite cells and one large nerve cell (D,N). Smaller neurons suggest a deficit of cytoplasmic ferroportin. The merged images of (C) and (D) confirm the proximity of neurons and ferroportin-bearing satellite cells (E). Bars, (A) and (B), 20  $\mu$ m; (C,D), 50  $\mu$ m.

in digests of DRG yielded  $25.4 \pm 10.3$   $\mu$ g/gram wet weight (mean  $\pm$  S.D.) in FA (n = 3) and  $28 \pm 13.4$   $\mu$ g/gram wet weight in controls (n = 8). The difference was not significant at  $\alpha = 0.05$  ( $p = 0.77$ ). Iron mapping by X-ray fluorescence confirmed the highest signal under the capsule of DRG and in association with the most abundant DRG neurons. Quantification of iron fluorescence did not show significant differences between FA and controls [14]. Despite normal iron levels in DRG of FA, immunofluorescence with antibodies to holoferitin and ferroportin suggest shifts in iron-related proteins [14]. In FA, ferritin fluorescence becomes very prominent in hyperplastic satellite cells and residual nodules (Fig. 9). Normal DRG also express ferroportin in neuronal cytoplasm and satellite cells. In FA, ferroportin immunofluorescence disappears from neurons but remains prominent in satellite cells and residual nodules (Fig. 10). The interpretation of these observations remains

difficult, but changes in ferritin and ferroportin expression in DRG of FA suggest iron dysmetabolism at the cellular level.

## 5. Conclusions

Many questions remain about iron in FA. The disease does not cause accumulation of total iron in any of the affected tissues. Nevertheless, the study of FA cardiomyopathy confirms iron in cardiomyocytes that undergo necrosis. It is unknown whether this process contributes to the clinical manifestations of heart disease in FA that include myocarditis and fibrosis. Fibrosis is more widespread than iron accumulation in a small percentage of heart fibers.

The destruction of the dentate nucleus in FA includes progressive atrophy of large nerve cells. The studies described here do not prove a role of iron in this process, and

the accumulation of iron and its surrogate marker ferritin in white matter oligodendroglia suggest a downstream effect of nerve cell atrophy.

The role of iron in DRG in FA is not readily explained. The apparent translocation of ferritin and ferroportin to perineuronal satellite cells points to iron dysmetabolism at the cellular level but does not clarify the overall role of iron in the pathogenesis of the DRG lesion in FA.

### Author Contributions

AHK designed the research study, made figures and wrote the manuscript.

### Ethics Approval and Consent to Participate

Not applicable.

### Acknowledgment

The author thanks the families of FA patients who over many years permitted autopsies to help research in this disease. Drs. Sonia Levi and Paolo Santambrogio generously donated anti-mitochondrial ferritin, and Dr Mitchell Knutson provided anti-ferroportin. The author also acknowledges the Veterans Affairs Medical Center in Albany, NY, USA, for providing access to a large laboratory. Dr. Joseph E. Mazurkiewicz, Albany Medical College, generated the double-label immunofluorescence images on his Zeiss LSM 880 laser scanning confocal microscope.

### Funding

National Institutes of Health (R01-NS069454) and Friedreich's Ataxia Research Alliance.

### Conflict of Interest

The author declares no conflict of interest.

### References

- [1] Lamarche JB, Côté M, Lemieux B. The cardiomyopathy of Friedreich's ataxia morphological observations in 3 cases. *The Canadian Journal of Neurological Sciences. Le Journal Canadien des Sciences Neurologiques*. 1980; 7: 389–396.
- [2] Campuzano V, Montermini L, Moltò MD, Pianese L, Cossée M, Cavalcanti F, *et al.* Friedreich's ataxia: autosomal recessive disease caused by an intronic GAA triplet repeat expansion. *Science* (New York, N.Y.). 1996; 271: 1423–1427.
- [3] Maio N, Jain A, Rouault TA. Mammalian iron-sulfur cluster biogenesis: Recent insights into the roles of frataxin, acyl carrier protein and ATPase-mediated transfer to recipient proteins. *Current Opinion in Chemical Biology*. 2020; 55: 34–44.
- [4] Waldvogel D, van Gelderen P, Hallett M. Increased iron in the dentate nucleus of patients with Friedreich's ataxia. *Annals of Neurology*. 1999; 46: 123–125.
- [5] Boddaert N, Le Quan Sang KH, Rötig A, Leroy-Willig A, Gallet S, Brunelle F, *et al.* Selective iron chelation in Friedreich ataxia: biologic and clinical implications. *Blood*. 2007; 110: 401–408.
- [6] Michael S, Petrocine SV, Qian J, Lamarche JB, Knutson MD, Garrick MD, *et al.* Iron and iron-responsive proteins in the cardiomyopathy of Friedreich's ataxia. *Cerebellum* (London, England). 2006; 5: 257–267.
- [7] Koeppen AH, Ramirez RL, Becker AB, Bjork ST, Levi S, Santambrogio P, *et al.* The pathogenesis of cardiomyopathy in Friedreich ataxia. *PLoS ONE*. 2015; 10: e0116396.
- [8] Perls M. Nachweis von Eisenoxyd in gewissen Pigmenten. *Virchows Archiv für Pathologische Anatomie und Physiologie und für Klinische Medizin*. 1867; 39: 42–48. (In German)
- [9] Koeppen AH, Michael SC, Knutson MD, Haile DJ, Qian J, Levi S, *et al.* The dentate nucleus in Friedreich's ataxia: the role of iron-responsive proteins. *Acta Neuropathologica*. 2007; 114: 163–173.
- [10] Koeppen AH, Ramirez RL, Yu D, Collins SE, Qian J, Parsons PJ, *et al.* Friedreich's ataxia causes redistribution of iron, copper, and zinc in the dentate nucleus. *Cerebellum* (London, England). 2012; 11: 845–860.
- [11] Spatz H. Über den Eisennachweis im Gehirn, besonders in Zentren des extrapyramidal-motorischen Systems. *Zeitschrift für die gesamte Neurologie und Psychiatrie*. 1922; 77: 261–390. (In German)
- [12] Koeppen AH, Becker AB, Qian J, Feustel PJ. Friedreich Ataxia: Hypoplasia of Spinal Cord and Dorsal Root Ganglia. *Journal of Neuropathology and Experimental Neurology*. 2017; 76: 101–108.
- [13] Koeppen AH, Morral JA, Davis AN, Qian J, Petrocine SV, Knutson MD, *et al.* The dorsal root ganglion in Friedreich's ataxia. *Acta Neuropathologica*. 2009; 118: 763–776.
- [14] Koeppen AH, Kuntzsch EC, Bjork ST, Ramirez RL, Mazurkiewicz JE, Feustel PJ. Friedreich ataxia: metal dysmetabolism in dorsal root ganglia. *Acta Neuropathologica Communications*. 2013; 1: 26.